# Unraveling the hydrolysis of $\beta$-1,4-glycosidic bond in cello-oligosaccharides over carbon catalysts

Pengru Chen, [a,b] Abhijit Shrotri, [a]* Atsushi Fukuoka [a]*

[a]Institute for Catalysis, Hokkaido University, Kita 21 Nishi 10, Kita-ku, Sapporo, Hokkaido 001-0021, Japan

[b]Graduate School of Chemical Sciences and Engineering, Hokkaido University, Kita 13 Nishi 8, Kita-ku, Sapporo, Hokkaido 060-8628, Japan

**Abstract**: Carbon catalysts having weakly acidic groups are uniquely active for hydrolysis of cellulose to produce cello-oligosaccharides and glucose. Although adsorption of cellulose molecules on carbon is attributed as the cause for this behavior, the effect of adsorption on the reaction is not well understood. In order to understand the underlying mechanism, we investigated the hydrolysis of cello-oligosaccharides with varying chain length over different catalyst. Carbon catalysts favored hydrolysis of larger oligosaccharides with an 11-fold increase in reaction rate constant from cellobiose to cellohexaose. Activation energy required to cleave the glycosidic bonds reduced concurrently with increase in molecule size. Based on these data, in conjugation with the

stronger affinity of adsorption for larger oligosaccharides, we propose that axial adsorption within the micropores of carbon causes conformational change in the structure of cello-oligosaccharide molecules, resulting in reduction of activation energy required to cleave the $\beta$-1,4-glycosidic bonds. Consequently, this translates to higher rate of reaction for larger cello-oligosaccharides and explains the high reactivity of carbon catalyst towards cellulose hydrolysis.

# Introduction

Cellulose, the primary component of lignocellulosic biomass, is the most abundant carbon-based renewable resource on our planet. It is a biopolymer composed of anhydro-glucose units linked by $\beta$-1,4-glycosidic bonds.[1,2] Catalytic hydrolysis of the $\beta$-1,4-glycosidic bonds in cellulose is a crucial step in producing biofuels and value-added chemicals, which can reduce the dependence on fossil fuels and petroleum industry.[3-5]

Enzymes[6-8] and acid catalysts[9-12] are effective for hydrolysis of cellulose to oligosaccharides and glucose. Partial hydrolysis produces water-soluble cello-oligosaccharides as major component,[13,14] which possess the repeated $\beta$-1,4-glycosidic linkages but have a low degree of polymerization (DP). These oligosaccharides exhibit biological activity that can benefit the growth and health of plants, animals, and humans.[15-17] Complete hydrolysis of cellulose produces glucose, a precursor for value-added chemicals and fuels.[18-21]

Carbon catalysts are most active for hydrolysis of cellulose among heterogeneous acid catalysts. They are also benign and do not contaminate the product solution, making them ideal for synthesis of cello-oligosaccharide for use in agriculture and healthcare industries.[9,22,23] Carbon catalysts bearing weakly acidic functional groups such as

hydroxyl (-OH) and carboxylic (-COOH) groups show comparatively high activity along with good hydrothermal stablity.[24,25] Owing to the insoluble nature of cellulose, a strong interaction between catalyst and cellulose is essential in a heterogeneous reaction. The polyaromatic surface of carbon catalyst can adsorb cellulose molecules by CH-π and hydrophobic interactions[26], and it is believed that this adsorption promotes the interaction between acidic functional groups and $\beta$-1,4-glycosidic bonds.[5] The DP of the adsorbed molecules can affect their adsorption capacity and larger oligosaccharides show higher affinity towards carbon surface.[26-28] Katz's group found that there was a monotonical decrease in free energy of adsorption with increase in the chain length of oligosaccharides over mesoporous carbon nanoparticles.[28] Our group observed a linear decrease in the adsorption enthalpy with an increase in chain length of oligosaccharides.[26]

The change in adsorption affinity with chain length of oligosaccharide can affect the selectivity of cello-oligosaccharides produced during cellulose hydrolysis. In a previous study, we found that carbon can catalyze hydrolysis of cellulose in a semi-flow reactor to yield cello-oligosaccharides without forming large amounts of glucose. The distribution of DP, determined by quantitative MALDI-TOF MS analysis, suggested a decrease in rate of hydrolysis as the reaction progressed.[29] However, there is a lack of holistic understanding about the dependence of molecule size on the rate of hydrolysis and the influence of adsorption during reaction. Therefore, fundamental approach towards assessing the change in rate of hydrolysis from a kinetic and mechanistic perspective is essential to determine the underlying factors responsible for high activity of carbon catalysts.

In this study, we report the hydrolysis of a series of cello-oligosaccharides in the presence of heterogeneous and homogeneous catalysts. Kinetic analysis is done to compare the change in rate of hydrolysis over different catalysts. Investigation on the adsorption affinity of oligosaccharides along with determination of apparent activation energy are used to ascertain the factors responsible for change in hydrolysis rate. Based on the experimental results, we propose a plausible mechanism which explains the hydrolysis behavior of large cellulose molecules over carbon catalysts.

# Experimental section

## Materials

Activated carbon (denoted as AC) was supplied from Ajinomoto Fine-Techno (volume mean diameter = 42 μm). Amberlyst 70 (0.4 – 0.8 mm) was purchased from Organo Corporation. H-beta was supplied from Catalysis Society of Japan. Cellotriose (G3, 95 %), cellotetraose (G4, 95 %), cellopentaose (G5, 95 %) and cellohexaose (G6, 94 %) were purchased from Megazyme. Glucose and cellobiose were purchased from Kanto Chemical Industries. 1,6-Hexanediol and sulfuric acid ($H_2SO_4$, 98 %) were purchased from Wako Pure Chemical Industries. DMSO was obtained from Tokyo Chemical Industry.

## Air oxidation of carbon catalyst

Air oxidation of carbon was performed using a method reported previously.[29] Briefly, activated carbon AC (4.0 g) was spread on a Pyrex dish of diameter 130 mm with a uniform thickness. The sample was then heated in a muffle furnace under air with the following program: 298 to 393 K at a rate of 10 K $min^{-1}$ and then maintained at 393 K for 2 h to remove the physisorbed water, followed by heating to 698 K at a rate of 4 K $min^{-1}$

and then maintaining at 698 K for further 10 h. The oxidized carbon catalyst was denoted as AC-Air. AC-Air-L was prepared via the same method by lowering the oxidation temperature to 673 K.

## Characterization of catalyst

Specific surface area of solid catalysts was determined by $N_2$ adsorption-desorption measurement (BEL Japan, BELSORP-mini) after vacuum drying at 393 K for 3 h. The total amount of acidic functional groups on solid catalysts were calculated by the titration.[30] The acidity of H-beta catalyst was also quantified by $NH_3$-temprature programmed desorption (TPD) (BEL Japan, BELCAT-A coupled with a mass spectrometer).

## Catalytic reactions

Hydrolysis of cello-oligosaccharides was performed in a glass tube placed inside a pressure-resistant hastelloy reactor (5 mL, TVS-1). For a typical reaction, 0.5 mL of water containing 1 μmol of cello-oligosaccharide substrate was added to the glass tube along with 5 mg of solid catalyst (in the case of $H_2SO_4$, 6.4 μmol of acid was used to replicate the acid content of 5 mg of AC-Air) and a magnetic stirrer bar. The glass tube was then placed in the reactor. The setup was purged and then pressurized to 0.5 MPa with argon (Ar) before immersing into a heated oil bath for a set period of time. After reaction, the reactor was cooled to room temperature and 0.1 mL of water containing 1 μmol of 1,6-Hexanediol was added to the mixture to serve as internal standard. The catalyst was separated from the reaction mixture by centrifugation and then washed three times with DMSO (1 mL) to extract adsorbed sugar molecules. The reaction solution and the liquids obtained after washing were mixed and diluted to 5 mL using a volumetric flask. This

obtained solution was analyzed to calculate the concentration of oligosaccharides by using a high-performance liquid chromatography (HPLC) system equipped with a refractive index detector (Shimadzu LC 10-ATVP) and a series of three Shodex Sugar SB 802.5HQ columns (ø 8 × 300mm; eluent, water 0.5 mL $min^{-1}$; 328 K).

### Adsorption of cello-oligosaccharides

Adsorption of oligosaccharides on solid catalysts was performed at room temperature. Solid catalyst (5 mg) was added to a vial containing 0.5 mL aqueous solution of adsorbate. The mixture was equilibrated under stirring for a period of 30 min which was sufficient to reach the adsorption equilibrium (Fig. S1). The sample was subsequently filtrated, and the solution was analyzed by the HPLC system described above. The amount of substrate adsorbed was calculated as the difference of sugar concentration in the liquid phase before and after adsorption

## Results and discussion

### Characterization of Catalysts

Carbon catalysts containing weakly acidic functional groups were prepared by air-oxidation of activated carbon (named AC) at elevated temperature. Amberlyst 70 (sulfonated resin catalyst), H-beta zeolite and homogeneous $H_2SO_4$ were used for comparing the activity with carbon materials. The $N_2$-adsorption isotherms for solid catalysts is shown in Fig S2. The Brunauer–Emmett–Teller (BET) surface areas of carbon catalyst prepared by oxidation at 698 K (named AC-Air, burn-off 53 %) was calculated as 877 $m^2 g^{-1}$, which was lower than pristine AC (1143 $m^2 g^{-1}$) owing to collapse of some pores during the oxidation treatment (Table 1). AC-Air-L, a catalyst prepared by oxidation at milder condition (673 K, burn-off 30%), exhibited a similar surface area

(1214 $m^2 g^{-1}$) to AC because of lower degree of oxidation. Zeolite H-beta had a surface area of 607 $m^2 g^{-1}$, a value typical for zeolite catalysts. The $N_2$ adsorption over Amberlyst 70 was negligible as the resin catalyst is not porous. However, the resin is permeable to reactants in aqueous solution allowing access to the acid sites.[31] The number of acidic functional groups on catalysts were calculated by titration with NaOH.[30] Amberlyst 70 showed the highest number of acid functional groups (3172 μmol $g^{-1}$) originating from -$SO_3H$ groups. Acidic sites originating from carboxyl, hydroxyl and lactone groups are known to be present over oxidized carbon catalysts.[25] The total number of acidic functional groups in AC-Air and AC-Air-L was determined as 2560 μmol $g^{-1}$ and 2075 μmol $g^{-1}$, respectively. Lower oxidation temperature of AC-Air-L (673 K) introduced fewer functional groups as expected. Titration of H-beta showed a low concentration of acid sites of 296 μmol $g^{-1}$, consistent with the value (299 μmol $g^{-1}$) quantified using $NH_3$-TPD.

Table 1: BET surface area and number of acid sites on solid acid catalysts.

| Catalyst | BET surface area ($m^2 g^{-1}$) | Total number of acid sites (μmol $g^{-1}$) |
|---|---|---|
| AC | 1143 | 355 |
| AC-Air-L | 1214 | 2075 |
| AC-Air | 877 | 2560 |
| Amberlyst 70 | - | 3172 |
| H-beta zeolite | 607 | 296 |

## Cello-oligosaccharides hydrolysis

Hydrolysis of cello-oligosaccharide with DP ranging from 2 - 6 was performed in the presence of AC-Air at 413 K to investigate the influence of chain length on the rate of hydrolysis. For cellobiose (G2) hydrolysis, 46 % conversion was achieved after 120 min of reaction (Fig. 1a). The hydrolysis pathway of cellobiose is shown in Scheme 1 and all steps were assumed to be first order reaction for kinetic analysis.[5,32] Accordingly, equations (1) – (4) were used to represent the hydrolysis of cellobiose and degradation of glucose:

$$\frac{d[G2]}{dt} = -k_2\,[G2] \qquad (1)$$

$$[G2] = [G2]_0 e^{-k_2 t} \qquad (2)$$

$$\frac{d[Glucose]}{dt} = -k_1\,[Glucose] + 2k_2\,[G2] \qquad (3)$$

$$[Glucose] = \frac{2k_2[G2]_0}{k_1 - k_2}\left(e^{-k_2 t} - e^{-k_1 t}\right) \qquad (4)$$

where [G2] and [Glucose] are concentrations of respective compounds. $[G2]_0$ is the initial concentration of cellobiose. *t* is the reaction time, and *k* is the rate constant. The rate constant $k_2$ for hydrolysis of cellobiose was determined as 0.38 $h^{-1}$ (Fig. 1f) by simulating equation (2) to fit the experimental data. Similarly, the rate constant for degradation of glucose ($k_1$) to other products was calculated as 0.03 $h^{-1}$. The high $k_2/k_1$ ratio indicated that the decomposition of glucose under the reaction condition was limited.

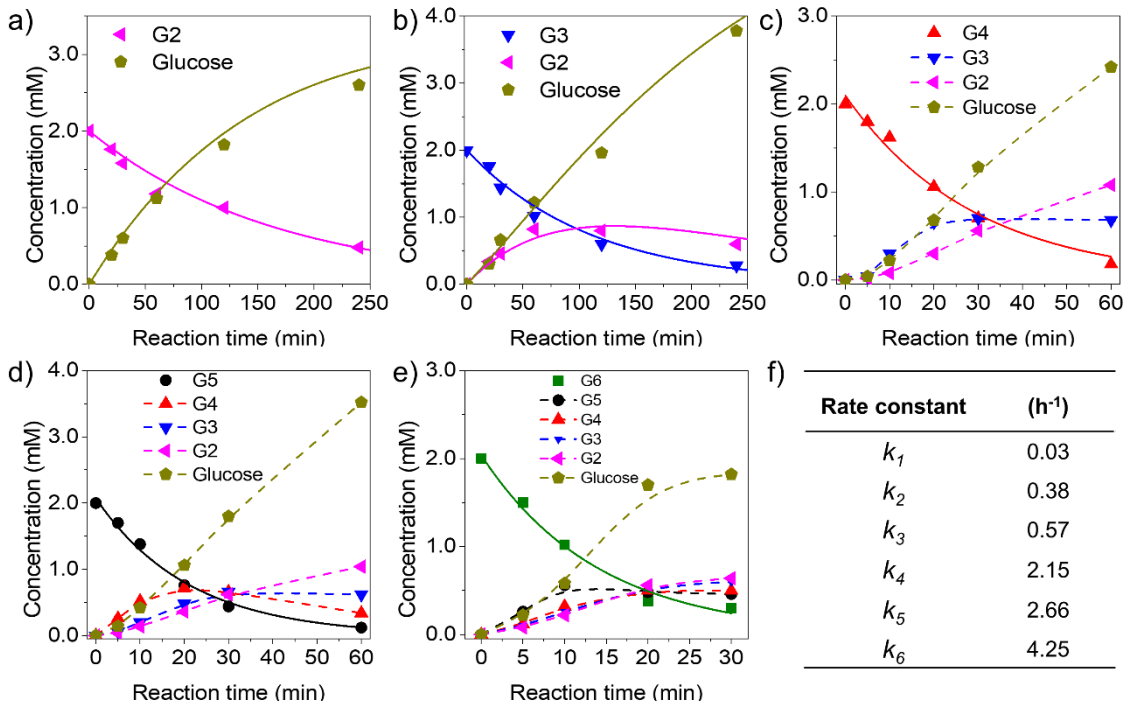


| Rate constant | ($h^{-1}$) |
|---|---|
| $k_1$ | 0.03 |
| $k_2$ | 0.38 |
| $k_3$ | 0.57 |
| $k_4$ | 2.15 |
| $k_5$ | 2.66 |
| $k_6$ | 4.25 |

**Fig. 1** Time dependent conversion of oligosaccharides and evolution of products in the presence of AC-Air. a) G2, b) G3, c) G4, d) G5, e) G6, f) Rate constant for hydrolysis of each cello-oligosaccharide. Reaction conditions: 1 μmol cello-oligosaccharides (G2-G6), 5 mg AC-Air, 0.5 mL $H_2O$, 0.5 MPa Ar, 413 K. Symbols denote experimental data points. Solid lines represent simulation of reaction using calculated rate constant and corresponding equations. Dashed lines show experimental trend for concentration of products during reaction.

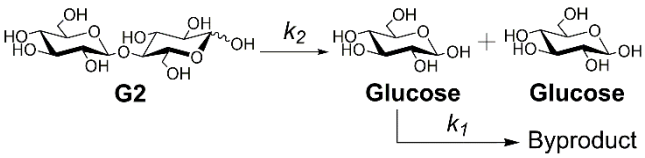


**Scheme 1.** Reaction pathway during hydrolysis of cellobiose.

Hydrolysis of cellotriose (G3) under the same reaction condition was faster than that of cellobiose and 50 % conversion was achieved in 60 min. The hydrolysis of

cellotriose to cellobiose and its further hydrolysis to glucose is shown in Scheme 2. The degradation of glucose to by-products was ignored owing to the very low value of $k_1$ estimated previously. Therefore, the hydrolysis rate constant $k_3$ was evaluated by the following rate equations (5) and (6).

$$\frac{d[G3]}{dt} = -k_3\,[G3] \qquad (5)$$

$$[G3] = [G3]_0 e^{-k_3 t} \qquad (6)$$

The rate constant $k_3$ for hydrolysis of cellotriose was calculated as 0.57 $h^{-1}$. Simulation of reaction profile by equations (6), (8) and (10) along with values of $k_2$ and $k_3$ fitted well with the experimental data (Fig. 1b).

$$\frac{d[G2]}{dt} = -k_2\,[G2] + k_3\,[G3] \qquad (7)$$

$$[G2] = \frac{k_3[G3]_0}{k_2 - k_3}\left(e^{-k_3 t} - e^{-k_2 t}\right) \qquad (8)$$

$$\frac{d[Glucose]}{dt} = 2k_2\,[G2] + k_3\,[G3] \qquad (9)$$

$$[Glucose] = [G3]_0\left\{\frac{(k_3 - 3k_2)e^{-k_3 t} + 2k_3 e^{-k_2 t}}{k_2 - k_3} + 3\right\} \qquad (10)$$

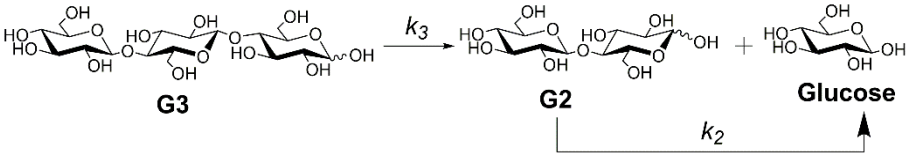


**Scheme 2**. Reaction pathway during hydrolysis of cellotriose.

Based on the good fit of rate equations for G2 and G3, the rate equation for hydrolysis of cello-oligosaccharide was generalized:

$$\frac{d[Gx]}{dt} = -k_x\,[Gx] \qquad (11)$$

$$[Gx] = [Gx]_0 e^{-k_x t} \qquad (12)$$

where Gx represents the cello-oligosaccharide with a DP of x and $k_x$ represents the rate constant for hydrolysis of that cello-oligosaccharide.

The hydrolysis of cellotetraose (G4) was even faster (Fig. 1c) and $k_4$ was calculated as 2.15 $h^{-1}$. Furthermore, the rate constants for hydrolysis of cellopentaose (G5) and cellohexaose (G6) were calculated as 2.66 $h^{-1}$ and 4.25 $h^{-1}$, respectively (Fig. 1d and 1e). Consequently, kinetic analysis reveals that the rate of hydrolysis of cello-oligosaccharide increases dramatically with respect to its DP.

To ascertain if the increase in rate of hydrolysis is caused by a favorable interaction between cello-oligosaccharide and carbon catalyst or it is an inherent property of cello-oligosaccharides, we performed the hydrolysis of these compounds over other heterogeneous catalysts (Fig. 2). The time course for hydrolysis of cello-oligosaccharides over Amberlyst 70 is shown in Fig. S3. The rate constant for hydrolysis of cellobiose on Amberlyst 70 was much higher (1.05 $h^{-1}$) in comparison to AC-Air (0.38 $h^{-1}$) owing to the higher abundance of acid sites along with high acid strength of -$SO_3H$ group. However, unlike AC-Air, the rate constant for hydrolysis on Amberlyst 70 was not positively affected by increase in DP. In contrast, the rate constant gradually decreased with an increase in the chain length of cello-oligosaccharides. H-beta showed a significantly lower activity for the hydrolysis of cello-oligosaccharides (Fig. S4) and the rate constant was not influenced by increase in DP. The reaction rate in the presence of H-beta was not much different in comparison to a non-catalytic reaction (Fig. 2), suggesting the inability of H-beta zeolite to interact with cello-oligosaccharides.

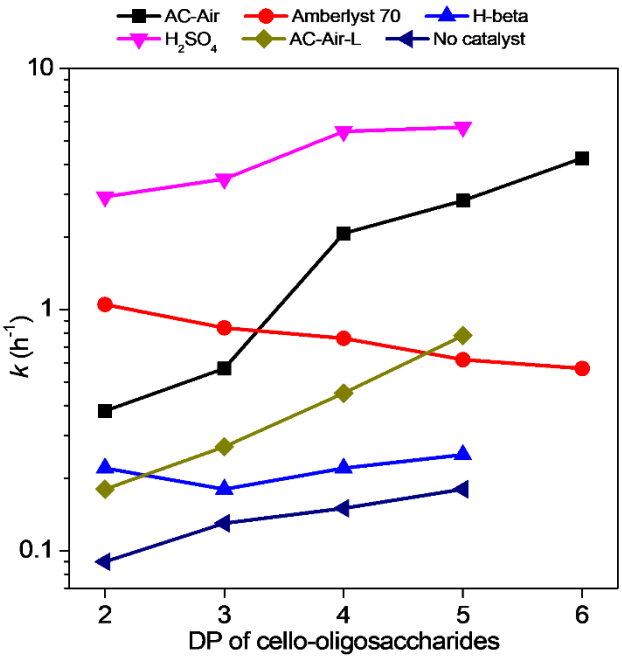


**Fig. 2** Comparison of change in rate constant for hydrolysis of cello-oligosaccharides in the presence of various acid catalysts. Reaction conditions: 1 μmol cello-oligosaccharides (G2-G6), 5 mg solid catalyst or 6.4 μmol $H_2SO_4$, 0.5 mL $H_2O$, 0.5 MPa Ar, 413 K.

We also evaluated the rate constant of cello-oligosaccharide hydrolysis in the presence of homogeneous $H_2SO_4$ catalyst (Fig. S5). The amount of $H_2SO_4$ used as catalyst was adjusted to match the total number of acid sites when AC-Air was used for the reaction. Hydrolysis in the presence of $H_2SO_4$ was much faster owing to its low pKa and homogeneous nature. The rate constant for hydrolysis of cellobiose was 2.94 $h^{-1}$, a value 7.7 times higher than that for AC-Air. A slight increase in rate constant of hydrolysis over $H_2SO_4$ was also observed with increasing DP of cello-oligosaccharides. However, the change in rate constant with DP was only 2.1 times from cellobiose to cellopentaose in comparison to 7 times for AC-Air.

The rate of hydrolysis over AC-Air-L was lower than that for AC-Air for all oligosaccharides due to the less amounts of functional groups on the surface. However, a

similar increasing trend for rate constant with DP of cello-oligosaccharide was obtained for AC-Air-L. From these results, we conclude that carbon materials show a uniquely preferential interaction with cello-oligosaccharides and the increase in DP favors this interaction causing an increase in their rate of hydrolysis.

It can be argued that the hydrolysis rate increased due to presence of more $\beta$-1,4-glycosidic linkages per molecule for larger cello-oligosaccharides. For example, cellobiose contains one glycosidic linkage whereas four linkages are present in cellopentaose. However, the rate constant increased 7 times from cellobiose to cellopentaose in the presence of AC-Air, a value well above the increase in number of glycosidic linkages. Moreover, if the number of glycosidic linkages plays a crucial role, then its effect should be more prominent in the presence of $H_2SO_4$. However, the increase in rate constant was only 2.1 times in this case. This discrepancy further confirms the inherent ability of carbon catalysts to easily hydrolyze cello-oligosaccharides with higher degree of polymerization.

## Adsorption of cello-oligosaccharides over solid catalysts

One distinct property of carbon materials is their ability to adsorb carbohydrates, which is likely to influence the rate of hydrolysis. It has been clarified that the adsorption of $\beta$-1,4-glucans on carbon surface occurs by CH-$\pi$ and hydrophobic interactions.[26,28] Hydrolysis of cellulose is known to increase by 13 times when it is adsorbed on carbon surface by ball milling.[33] Therefore, we evaluated the adsorption of cello-oligosaccharides on all catalysts in our study at room temperature to elucidate its influence on rate of hydrolysis. Adsorption under reaction condition is expected to be

lower than room temperature, but the change in adsorption capacity with respect to cello-oligosaccharide size is expected to the follow the same trend.[26]

H-beta showed no adsorption of cello-oligosaccharides even though it had a relatively large surface area with micropores structure. The same phenomenon was observed in the case of Amberlyst 70 and there was no difference in the concentration of cello-oligosaccharides during adsorption.

The adsorption of cello-oligosaccharides on AC-Air was markedly different. The adsorption isotherms for G2-G5 oligosaccharides over AC-Air are shown in Fig. 3a. They fitted well with the Langmuir adsorption model of type I isotherms in which the adsorption increased initially with change in concentration of reactant and then plateaus once the adsorption capacity was reached.[26,28] Accordingly, Langmuir formula shown in equation (13) was used to calculate the adsorption capacity ($Q_{max}$) and adsorption equilibrium constant ($K_{ads}$):

$$\frac{C}{Q_e} = \frac{1}{Q_{max}} C + \frac{1}{K_{ads} Q_{max}} \quad (13)$$

where $C$ is the equilibrium concentration of cello-oligosaccharides after adsorption, $Q_e$ (mg g $_{\text{adsorbent}}^{-1}$) and $Q_{max}$ (mg g $_{\text{adsorbent}}^{-1}$) are the adsorption amount and the maximum adsorption capacity of cello-oligosaccharides, respectively. $K_{ads}$ represents the adsorption equilibrium constant.

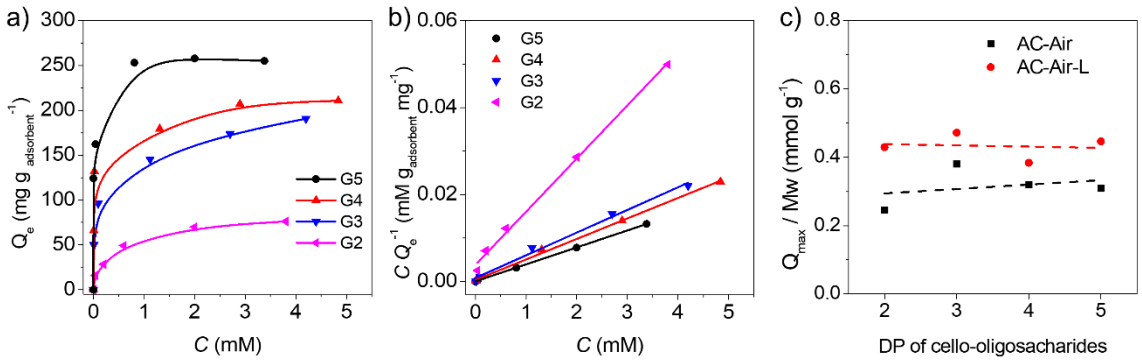


**Fig. 3** Adsorption of cello-oligosaccharides (G2-G5) on AC-Air: a) Adsorption isotherms, b) Langmuir plot derived from equation (13). c) Plot showing maximum molar concentration of oligosaccharides over AC-Air and AC-Air-L at saturation.

The Langmuir plots for each cello-oligosaccharide resulted in a good linear fit (Fig. 3b) and the calculated values for $Q_{max}$ and $K_{ads}$ are summarized in Table 2. The $Q_{max}$ for cellobiose was 84 mg $g_{adsorbent}^{-1}$, which increased sequentially to 256 mg $g_{adsorbent}^{-1}$ for cellopentaose. Similarly, the $K_{ads}$ also increased 40-fold from G2 to G5. These parameters indicate that there is a stronger affinity for adsorption of larger cello-oligosaccharides on carbon surface. AC-Air-L showed higher $Q_{max}$ and $K_{ads}$ for all cello-oligosaccharides in comparison to AC-Air. AC-Air-L is expected to have a higher polyaromatic surface owing to lower number of acidic functional groups and a larger surface area, which explains its higher adsorption capacity.

**Table 2** Langmuir constants of cello-oligosaccharide adsorption over carbon catalysts at room temperature.

| Substrate | AC-Air | | AC-Air-L | |
|---|---|---|---|---|
| | $Q_{max}$ (mg $g^{-1}$) | $K_{ads}$ ($M^{-1}$) | $Q_{max}$ (mg $g^{-1}$) | $K_{ads}$ ($M^{-1}$) |
| G2 | 84 | 2429 | 147 | 4000 |

| | | | | |
|---|---|---|---|---|
| G3 | 192 | 6500 | 238 | 42000 |
| G4 | 213 | 15667 | 256 | 195000 |
| G5 | 256 | 97500 | 370 | - |

Fig. 3c shows a plot of number moles of oligosaccharides adsorbed over carbon materials with respect to DP under saturation adsorption condition. For both carbon catalysts the total molar adsorption of oligosaccharides was not influenced with DP. Analysis of adsorption data reported by previous studies also shows that equivalent molar adsorption occurs over other carbon materials. Over K26, an alkali activated carbon, the molar adsorption of cellobiose and cellotriose was calculated as 1.2 and 1.0 mmol $g^{-1}$.[26] Similarly, over a mesoporous carbon surface the molar adsorption for cellobiose, cellotriose and cellotetraose was calculated as 1.6, 1.1 and 1.0 mmol $g^{-1}$.[28] Therefore, we conclude that although larger oligosaccharides show a higher affinity to adsorb over carbon surface, this doesn't influence the surface concentration of oligosaccharides and this phenomenon is not linked with the type of carbon material used. Hence the increase in rate of hydrolysis cannot simply be a result of higher abundance of larger oligosaccharide over the catalyst surface owing to stronger adsorption.

## Affinity of cello-oligosaccharides and carbon catalyst

Adsorption can also influence the structure of large molecules, especially when they are adsorbed within narrow pores. To examine this possibility, we compared the microporous structure of carbon materials with the size of cello-oligosaccharide molecules. The external surface area of AC-Air calculated by t-plot was only 45 $m^2 g^{-1}$. AC-Air-L had a similar structure with an external surface area of 55 $m^2 g^{-1}$. These surface

areas are much lower than the minimum surface area required for adsorption of oligosaccharides under equilibrium condition. This leads us to conclude that although adsorption may occur at any available surface area, the bulk of the cello-oligosaccharides are adsorbed within the micropores.

The pore size distribution of carbon catalysts was determined by NLDFT simulation (Fig. 4). AC-Air and AC-Air-L catalysts showed a presence of micropores smaller than 2.0 nm, with the peaks centered at 0.98 nm and 1.0 nm, respectively. Their distributions of pore width became broader compared to pristine AC. In comparison, the cellobiose molecule has dimensions of 1.0×0.8×0.6 nm, whereas cellopentaose has dimensions of 2.5×0.7×0.6 nm. Therefore, the cello-oligosaccharides, especially the larger ones, must axially enter the micropores and adsorb within the micropore of the carbon catalysts.

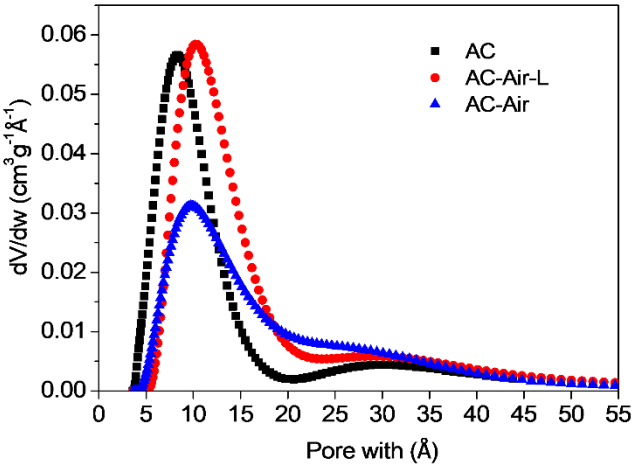


**Fig. 4** Pore size distribution of pristine and oxidized carbons determined by NLDFT simulation of $N_2$ adsorption isotherms.

The evolution of products during hydrolysis confirms this assertion. A closer inspection of hydrolysis data for cellotetraose (Fig. 5a) shows that the concentration of cellotriose was same as glucose within the first 10 mins of reaction, which was twice than that of cellobiose. Preferential hydrolysis of terminal glycosidic bonds would cause a

higher concentration of cellotriose and glucose (Figure 5d). Axial adsorption of oligosaccharides would favor the hydrolysis of terminal glycosidic bonds. A similar trend was also observed in the cases of hydrolysis of cellopentaose (Fig. 5b) and cellohexaose (Fig. 5c), in which cellotetraose and cellopentaose appeared as primary products along with equal amount of glucose. This observation is uniquely analogous to exoglucanase enzymes that sequentially cleave a glucose or cellobiose molecules from the chain end of cellulose.[34] Hence we can claim that the notion of heterogenous carbon catalysts randomly cleaving the β-1,4 glycosidic bonds of adsorbed cellulose molecules, in a manner analogues to endoglucanase, is not entirely true.

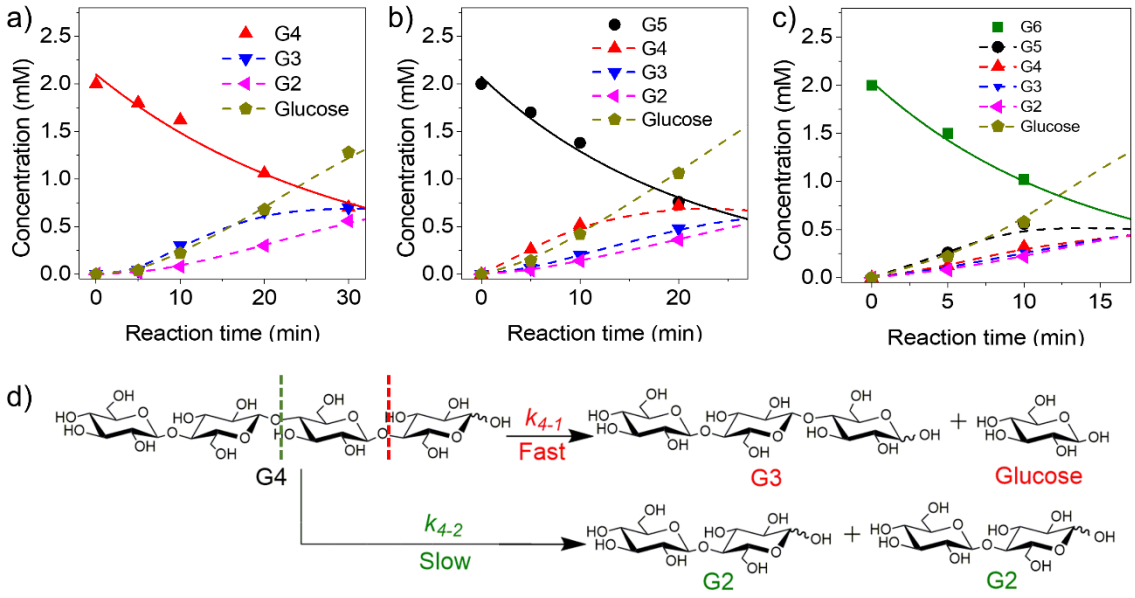


**Fig.** 5 Close up of reaction profiles shown in Fig. 1 to illustrate the evolution of products from a) G4, b) G5, c) G6 over AC-Air catalyst. d) Scheme showing the pathway for hydrolysis of either the terminal glycosidic linkages or the internal glycosidic linkage in G4.

## Activation energy of cello-oligosaccharides

Nevertheless, the axial adsorption and sequential cleavage of oligosaccharides also does not fully explain the increase in rate of hydrolysis. So we evaluated the change in apparent activation energy during hydrolysis of cello-oligosaccharides over AC-Air. Arrhenius equation for the calculation is shown in equation (14):

$$lnk = -\frac{E_a}{R}\frac{1}{T} + lnA \qquad (14)$$

where $k$ ($h^{-1}$) is the rate constant of cello-oligosaccharide hydrolysis, $E_a$ (kJ $mol^{-1}$) represents the activation energy for cello-oligosaccharides hydrolysis. $A$ ($h^{-1}$) and $T$ (K) are the pre-exponential factor for the reaction and the absolute reaction temperature, respectively. $R$ (kJ $K^{-1}$ $mol^{-1}$) is the universal gas constant.

Hydrolysis of cello-oligosaccharides at other temperatures also conformed to the pattern of increase in rate constant with increase in number of glycosidic bonds (Table 3, Fig. S6-8). The Arrhenius plots of these data fitted linearly with a high correlation coefficient (0.99, Fig. 6). The apparent activation energy for cellobiose hydrolysis was calculated as 100 kJ $mol^{-1}$. A similar value of activation energy for cellotriose was obtained as 98 kJ $mol^{-1}$. The activation energy for hydrolysis of cellotetraose was 87 kJ $mol^{-1}$ which further decreased to 77 kJ $mol^{-1}$ for cellopentatose. This drastic reduction in the activation energy suggests a decrease in energy required to cleave the glycosidic bonds as the DP increases. Furthermore, it might be expected that the stronger adsorption of larger oligosaccharides would lead to an increase in the pre-exponential factor (*A*). Instead, the value of *A* decreased, which could be attributed to the *compensation effect* observed when comparing $E_a$ and *A* for reactions under similar conditions.[35]

**Table 3** Rate constant of cello-oligosaccharide hydrolysis at varying temperatures over AC-Air and the calculated activation energy of hydrolysis for respective compounds.

| Substrate | $k$ ($h^{-1}$) | | | | $E_a$ | $A$ |
|---|---|---|---|---|---|---|
| | 403 K | 413 K | 423 K | 433 K | (kJ $mol^{-1}$) | ($h^{-1}$) |
| G2 | 0.17 | 0.38 | 0.72 | 1.38 | 100 | $1.74 \times 10^{12}$ |
| G3 | 0.33 | 0.57 | 1.44 | 2.64 | 98 | $1.71 \times 10^{12}$ |
| G4 | 0.81 | 2.15 | 3.37 | 5.13 | 87 | $2.16 \times 10^{11}$ |
| G5 | 1.43 | 2.66 | 4.57 | 6.91 | 77 | $1.10 \times 10^{10}$ |

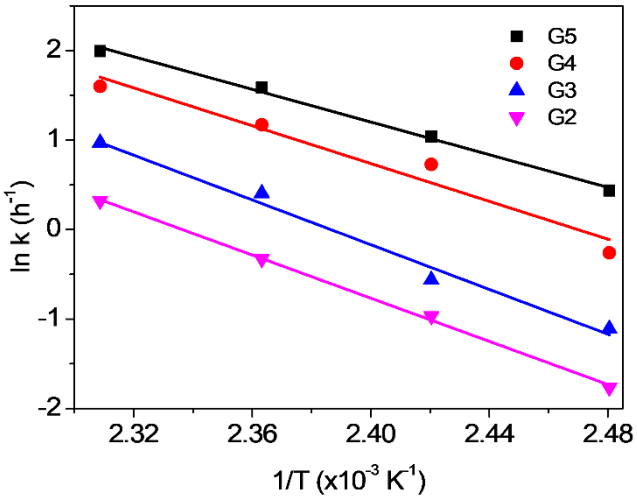


**Fig. 6** Arrhenius plot of cello-oligosaccharides (G2-G5) hydrolysis on AC-Air.

Moreover, we further calculated the activation energy under the same reaction condition in the presence of $H_2SO_4$ catalyst (Fig. S9-11). The Arrhenius plots and calculated values of activation energy are shown in Fig. S12. An identical value of 100 kJ $mol^{-1}$ for activation energy of cellobiose hydrolysis was observed.[†] A slight decrease in activation energy was also detected with the increase of DP of cello-oligosaccharides. However, the activation energy decreased only by 11 kJ $mol^{-1}$ from cellobiose to cellopentaose for $H_2SO_4$.

## Proposed hydrolysis mechanism

Based on the above observations and in light of previous reports, we propose that in addition to the presence of oxygenated functional groups, the adsorption and conformational change within the micropore influence rate of hydrolysis for cello-oligosaccharide. The increase in rate of hydrolysis with DP is caused by a decrease in activation energy required for hydrolysis of $\beta$-1,4-glycosidic bonds owing to their adsorption within the micropores of carbon. It is likely that the axial adsorption of a large molecule such as cellopentaose inside the micropores of carbon would cause a conformational change in its structure.[36] Cello-oligosaccharides conform to a stable twisted ribbon structure in aqueous solution.[37] Upon adsorption, this structure would untwist to accommodate itself within the pores and to achieve adsorption of multiple glucose units over the carbon surface (Fig. 7). This deviation from the stable twisted form could cause a change in $\beta$-1,4-glycosidic bond angle, leading to reduction in activation energy required for its cleavage.

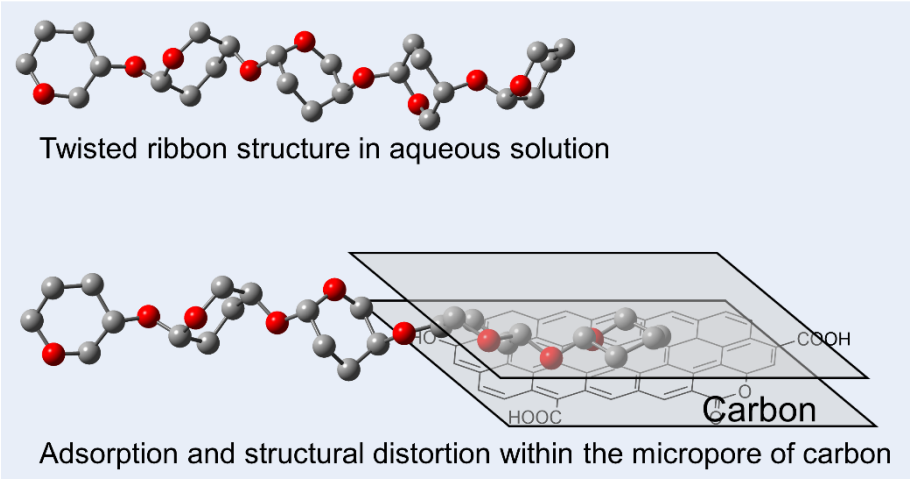


**Fig. 7** Illustration showing the twisted ribbon structure of cellopentaose in water and the proposed structural change during the adsorption on carbon surface. For clarity the

hydroxyl groups are not shown and only the pyranose rings are depicted linked by $\beta$-1,4-glycosidic bond.

## Conclusions

We performed hydrolysis of cello-oligosaccharides with increasing degree of polymerization in the presence of various catalysts. Only in the presence of carbon catalysts the rate of hydrolysis was strongly dependent on their degree of polymerization. The hydrolysis rate constant increased 11 times with an increase in DP from 2 to 6. A simultaneous decrease in apparent activation energy for hydrolysis was also observed with respect to increase in DP. In addition, the larger oligosaccharide showed a stronger affinity towards adsorption over the narrow micropores of the carbon surface. A preference for hydrolysis of terminal over internal glycosidic bonds was observed, which was analogous to some enzymes in the cellulase family. Based on these observations, we propose that the increase in rate of hydrolysis is caused by reduction in activation energy which is the result of conformational changes in the oligosaccharide molecules when they adsorb within micropores of carbon.

## Footnote

[†]This result was lower than previously reported value of 120-130 kJ $mol^{-1}$ for cellobiose hydrolysis over concentrated $H_2SO_4$.[5] Lower concentration of cellobiose in our reaction mixture (2 mM) was the reason for this low value because activation energy of 139 kJ $mol^{-1}$ was obtained when 50 mM solution of cellobiose was used in our reaction.

## Conflicts of interest

There are no conflicts to declare.

## Acknowledgements

This work was supported by the Japan Science and Technology Agency (JST) ALCA (JPMJAL1309). AS would like to acknowledge the funding support from Research Fund Program for Early Career Scientists from Hokkaido University.

## References

1. G. W. Huber, S. Iborra and A. Corma, *Chem. Rev.*, 2006, **106**, 4044-4098.

2. D. Klemm, B. Heublein, H.-P. Fink and A. Bohn, *Angew. Chem. Int. Ed.*, 2005, **44**, 3358-3393.

3. A. J. Ragauskas, C. K. Williams, B. H. Davison, G. Britovsek, J. Cairney, C. A. Eckert, W. J. Frederick, Jr., J. P. Hallett, D. J. Leak, C. L. Liotta, J. R. Mielenz, R. Murphy, R. Templer and T. Tschaplinski, *Science*, 2006, **311**, 484-489.

4. E. Kontturi, T. Tammelin and M. Osterberg, *Chem. Soc. Rev.*, 2006, **35**, 1287-1304.

5. R. Rinaldi and F. Schüth, *ChemSusChem*, 2009, **2**, 1096-1107.

6. H. Zhao, C. L. Jones, G. A. Baker, S. Xia, O. Olubajo and V. N. Person, *J. Biotechnol.*, 2009, **139**, 47-54.

7. N. Kamiya, Y. Matsushita, M. Hanaki, K. Nakashima, M. Narita, M. Goto and H. Takahashi, *Biotechnol. Lett.*, 2008, **30**, 1037-1040.

8. Q. Chu, X. Li, Y. Xu, Z. Wang, J. Huang, S. Yu and Q. Yong, *Process Biochem.*, 2014, **49**, 1217-1222.

9. A. T. To, P. W. Chung and A. Katz, *Angew. Chem. Int. Ed.*, 2015, **54**, 11050-11053.

10. Y.-B. Huang and Y. Fu, *Green Chem.*, 2013, **15**, 1095-1111.

11. S. Suganuma, K. Nakajima, M. Kitano, D. Yamaguchi, H. Kato, S. Hayashi and M. Hara, *J. Am. Chem. Soc.*, 2008, **130**, 12787-12793.

12. A. Charmot, P.-W. Chung and A. Katz, *ACS Sustainable Chem. Eng.*, 2014, **2**, 2866-2872.

13. A. Martin-Mingot, K. D. O. Vigier, F. Jérômeb and S. Thibaudeau, *Org. Biomol. Chem.*, 2012, **10**, 2521-2524.

14. T. Liebert, M. Seifert and T. Heinze, *Macromol. Symp.*, 2008, **262**, 140-149.

15. T. Hasunuma, K. Kawashima, H. Nakayama, T. Murakami, H. Kanagawa, T. Ishii, K. Akiyama, K. Yasuda, F. Terada and S. Kushibiki, *Anim. Sci. J.*, 2011, **82**, 543-548.

16. C. D. A. Souza, S. Li, A. Z. Lin, F. Boutrot, G. Grossmann, C. Zipfel and S. C. Somerville, *Plant Physiol.*, 2017, **173**, 2383-2398.

17. E. Billès, V. Coma, F. Peruch and S. Grelier, *Polym. Int.*, 2017, **66**, 1227-1236.

18. A. Shrotri, H. Kobayashi and A. Fukuoka, *Acc. Chem. Res.*, 2018, **51**, 761-768.

19. X. Zhang, K. Wilson and A. F. Lee, *Chem. Rev.*, 2016, **116**, 12328-12368.

20. A. Onda, T. Ochi and K. Yanagisawa, *Green Chem.*, 2008, **10**, 1033-1037.

21. B. R. Caes, M. J. Palte and R. T. Raines, *Chem. Sci.*, 2013, **4**, 196-199.

22. A. Shrotri, H. Kobayashi and A. Fukuoka, *ChemCatChem*, 2016, **8**, 1059-1064.

23. G. S. Foo and C. Sievers, *ChemSusChem*, 2015, **8**, 534-543.

24. H. Kobayashi, T. Komanoya, K. Hara and A. Fukuoka, *ChemSusChem*, 2010, **3**, 440-443.

25. A. Shrotri, H. Kobayashi and A. Fukuoka, *ChemSusChem*, 2016, **9**, 1299–1303.

26. M. Yabushita, H. Kobayashi, J.-Y. Hasegawa, K. Hara and A. Fukuoka, *ChemSusChem*, 2014, **7**, 1443-1450.

27. P. Dornath, S. Ruzycky, S. Pang, L. He, P. Dauenhauer and W. Fan, *Green Chem.*, 2016, **18**, 6637-6647.

28. P. W. Chung, A. Charmot, O. M. Gazit and A. Katz, *Langmuir*, 2012, **28**, 15222-15232.

29. P. Chen, A. Shrotri and A. Fukuoka, *ChemSusChem*, 2019, **12**, 2576-2580.

30. H. P. Boehm, *Carbon*, 2002, **40**, 145-149.

31. J. Guilera, R. Bringué, E. Ramírez, M. Iborra and J. Tejero, *Ind. Eng. Chem. Res.*, 2012, **51**, 16525-16530.

32. L. Vanoye, M. Fanselow, J. D. Holbrey, M. P. Atkins and K. R. Seddon, *Green Chem.*, 2009, **11**, 390.

33. M. Yabushita, H. Kobayashi, K. Hara and A. Fukuoka, *Catal. Sci. Technol.*, 2014, **4**, 2312-2317.

34. K. Igarashi, T. Uchihashi, A. Koivula, M. Wada, S. Kimura, T. Okamoto, M. Penttil, T. Ando and M. Samejima, *Science*, 2011, **33**, 1279-1282.

35. W. C. Conner Jr., *J. Catal.*, 1982, **78**, 238-246.

36. P.-W. Chung, M. Yabushita, A. T. To, Y. Bae, J. Jankolovits, H. Kobayashi, A. Fukuoka and A. Katz, *ACS Catalysis*, 2015, **5**, 6422-6425.

37. M. Umemura, Y. Yuguchi and T. Hirotsu, *J. Phys. Chem. A*, 2004, **108**, 7063-7070.